

A new miniature, hand-held, solar-blind, reagentless standoff chemical, biological and explosives (CBE) sensor

W. F. Hug ^{*b}, R.D. Reid ^a, R. Bhartia ^b, A. L. Lane ^b

^a Photon Systems, Inc., 1512 Industrial Park St., Covina, CA 91722

^b Jet Propulsion Laboratory/Caltech, 4800 Oak Grove Dr., Pasadena, CA 91109

Abstract

Improvised explosive devices (IEDs), vehicle-borne improvised explosive devices (VBIEDs), and suicide bombers are a major threat to many countries and their citizenry. The ability to detect trace levels of these threats with a miniature, hand-held, reagentless, standoff sensor represents a major improvement in the state of the art of CBE surface sensors.

Photon Systems, Inc., in collaboration with Jet Propulsion Laboratory, recently demonstrated a new technology hand-held sensor for reagentless, close-range, standoff detection and identification of trace levels CBE materials on surfaces. This targeted ultraviolet CBE (TUCBE) sensor is the result of an Army Phase I STTR program. The resulting 5lb, 5W, flashlight-sized sensor can discriminate CBE from background materials using a combination of deep UV excited resonance Raman (RR) and laser induced native fluorescence (LINF) emissions resulting from excitation by a new technology deep UV laser. Detection and identification is accomplished in less than 1ms. Standoff excitation of suspicious packages, vehicles, persons, and other objects that may contain hazardous materials is accomplished using wavelengths below 250nm where Raman and native fluorescence emissions occupy distinctly different wavelength regions. This enables simultaneous detection of RR and LINF emissions with no interferences. The sensor employs fused RR/LINF chemometric methods to extract the identity of targeted materials from background clutter.

Photon Systems has demonstrated detection and identification of 100ng/cm² of explosives materials at a distance of 1 meter using a sensor with 3.8 cm optical aperture. Expansion of the optical aperture to 38 cm in a lantern-sized sensor will enable similar detection and identification of CBE materials at standoff distances of 10 meters. As a result of excitation and detection in the deep UV and the use of a gated detection system, the sensor is solar blind and can operate in full daylight conditions.

Keywords: deep UV Raman & native fluorescence; chemical, biological, and explosives detection and classification

1. INTRODUCTION

Several approaches are being developed for proximity or standoff detection and identification or classification of chemical, biological, and explosive hazards on surfaces. These include: standoff sensors with working distances of 10 m to 50 m using laser induced breakdown spectroscopic (LIBS) methods and being developed by several organizations using near IR lasers; and proximity sensors with working distances of a few mm to one cm using Raman spectroscopic (RS) methods and using 785 nm, 650 nm, and 532 nm lasers. There is also a sensor with working distance of 0.5 m to 1 m using resonance Raman spectroscopic (RRS) methods being developed using a 248 nm excimer laser at high data rates. Finally there is a new, miniature, sensor technology being developed by Photon Systems that has a working distance of 0.5 m to 10 m using a combination of RRS and laser induced native fluorescence (LINF) spectroscopic methods and using a new-technology 248.6 nm neon-copper (NeCu) transverse excited hollow cathode (TEHC) laser.

The new sensor, nominally called a targeted ultraviolet chemical, biological, and explosives (TUCBE) sensor, is the subject of this paper. This new sensor is designed for operation on small military robots, such as the IRobot PackBot EOD, or hand-held. The TUCBE sensor is nominally 5 lbs in weight and consumes less than 12 W from a battery or robot source. Similar sensors with the same components have been rated by the U.S. Army and NASA at technical readiness level (TRL) over 5.0 and versions of this sensor have been deployed on many expeditions to Antarctica, the Arctic, and the deep Ocean.

2. TUCBE SENSOR PERFORMANCE & CHRONOLOGY

Below are the preliminary specifications of the TUCBE sensor under development:

- Detects and classifies trace levels of CBE agents on surfaces.
- Reagentless: non-contact, non-destructive sensor for CBE agents without the need for any sample handling, preparation, or use of reagents or consumable material.
- Close-range standoff: performs detection in a range from 0.5 to 3.0 meters or more, dependent on concentrations
- Interrogation area: about 4mm diameter at 1m, 6mm diameter at 2m. Can be made smaller or larger if needed.
- Approximate Limits of Detection: 100 bacterial spores/cm² or 100ng/cm² explosives at standoff distance of 1 m with current Gen 1.0 sensor configuration. Gen 2.0 sensor projected to have these detection limits at 3 meters.
- Fast detection and analysis: performs detection, analysis, and classification of targets in less than one millisecond.
- Solar blind: performs detection in full daylight or room light conditions without compensation.
- Operator notification: Geiger mode audio and visual notification of hazard.
- Field or lab trainable: Sensor is field trainable and adaptable to varying applications and environments.
- Self-calibration: Sensor is self-calibrating to compensate for ambient temperature changes and/or degradation of components.
- Miniature size: 4" x 4" x 15" including laser, detectors, onboard data processing computer and all hardware, firmware and software needed to operate the sensor.
- Visible aiming beam: 532 nm DPSS laser aiming beam co-aligned with UV detector laser beam to enable easy identification of location of CBE information.
- Light weight: <8 lbs, including battery for hand held operation. Battery operation has been demonstrated for 8 hours with a small video camera battery.
- Power consumption: about 12W (24 VDC at 500mA)
- Target sample rate: up to about 20 Hz.
- Fast turn on: No preheating, warm-up or temperature regulation for laser. Only startup time is electronics and software startup.
- Rugged: all key components have been tested to 3X the launch and landing shock and vibration requirements for a mission to the planet Mars.
- Harsh environments: Lasers have been tested from -100°C to +60°C.
- Lifetime: 50 million data samples.

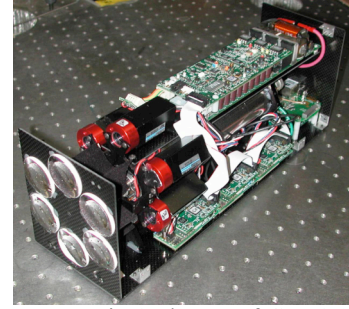


Fig.1. Photon of Gen 1.0 TUCBE sensor

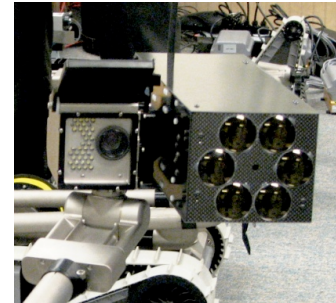


Fig.2. Photon of Gen 1.0 sensor on IRobot PackBot



Fig.3. Photon of Gen 2.0 hand-held sensor and use

During operation of the sensor, the deep UV laser is fired at a continuous rate up to about 20 Hz. During each laser pulse Raman and native fluorescence spectral information is collected and analyzed. Using this analysis we have demonstrated the ability to detect and differentiate both biological and explosive materials on a broad range of background surfaces including fabrics, painted and unpainted automobile body surfaces with and without overlays of interferant materials such as Arizona road dust, diesel fuel, soot, motor oil, and bacteria. Figure 4 shows this ability to differentiate materials where the various materials are shown in a 3 dimensional chemometric space based on Principal Component Analysis. The axes of this space are the first three principal components: PC1, PC2, and PC3. The explosive samples used for these tests were obtained from AccuStandard and the tests were done at a working distance of 1 m using the Gen 1.0 sensor which had a 38 mm diameter detection aperture for collecting the Raman and native fluorescence emissions from the target materials.

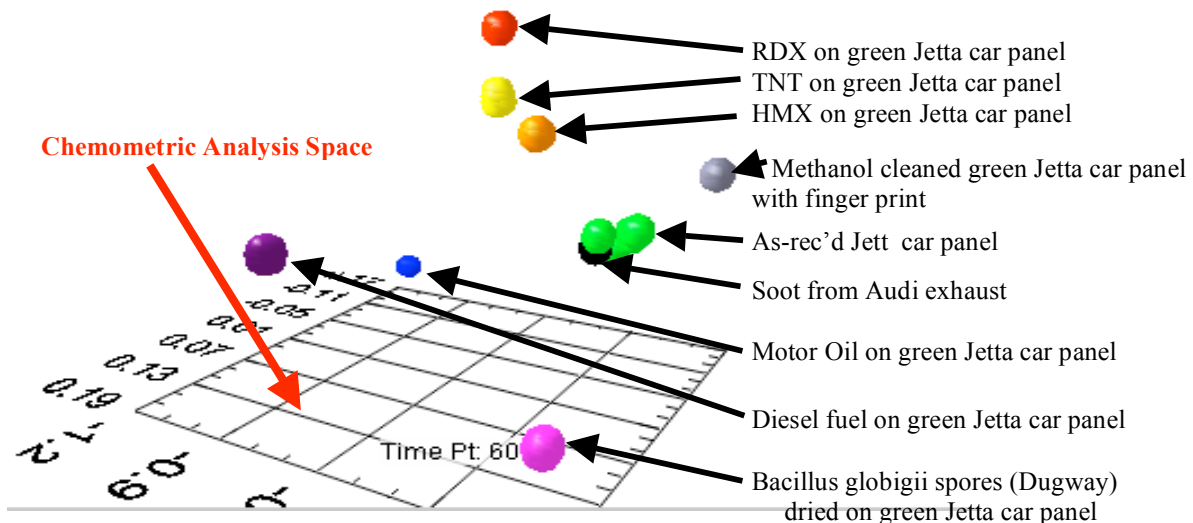


Fig.4. Illustration of chemical differentiability of a variety of explosive materials, bacteria, and background interferent materials. Explosives concentrations were 100 ng/cm².

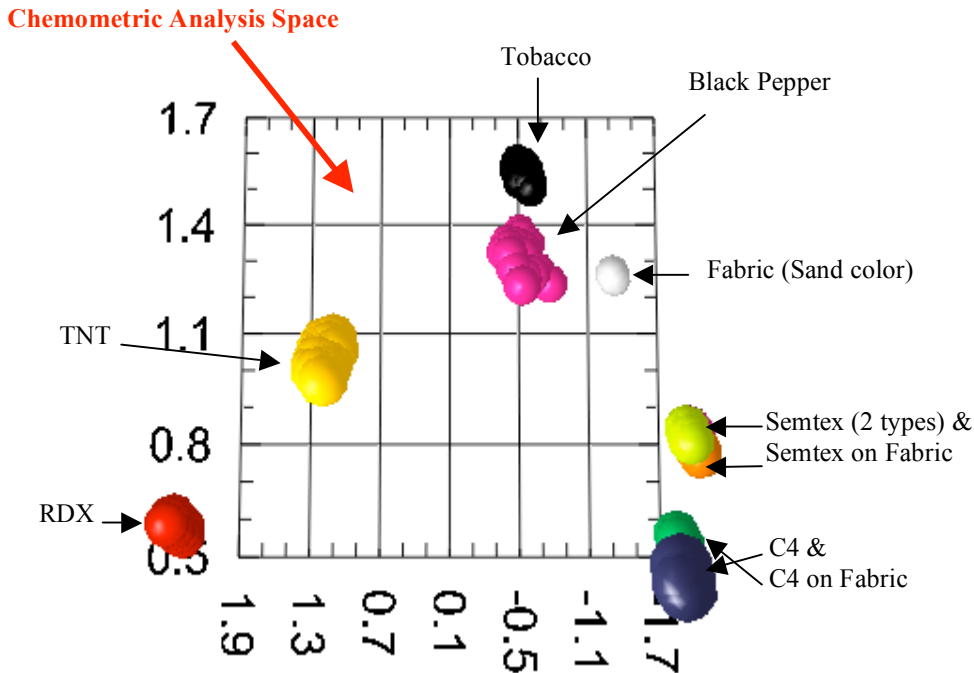


Fig. 5. Illustration of differentiability of military-grade explosives and interferents on a variety of backgrounds. Two different formulations were used for Semtex and C4.

Figure 5 shows the results of test of military-grade explosives and a variety of interferents such as tobacco and black pepper on different colored fabrics. Two different formulations of Semtex and C4 were tested and showed similar chemical signatures. These signatures are also clearly different from RDX, TNT, and the interferents pepper and tobacco.

When the sensor is aimed at a target and the laser is fired, a coordinate position in 3D PCA chemometric space, illustrated in Figs. 4 and 5 is determined. The association of this chemometric position to a specific chemical, background, or interferant material in the sensor's data base is determined by measuring the scalar distance, in chemometric space, of the unknown chemometric position to all known materials in the data base. The materials in the

data base are both pure and mixed materials and represent all that we know about an environment in which the sensor may be employed. Each time the laser is fired, a table of the most likely associations is listed in order of the proximity in chemometric space to the unknown. This is done for each laser pulse at a rate up to 20 Hz. Assuming the position of the laser focus is unchanged, the chemical identity is unchanged. Figure 6 is a photograph of the Gen 1.0 sensor aimed at a set of contaminants doped on a cardboard background at a distance of 1 m.

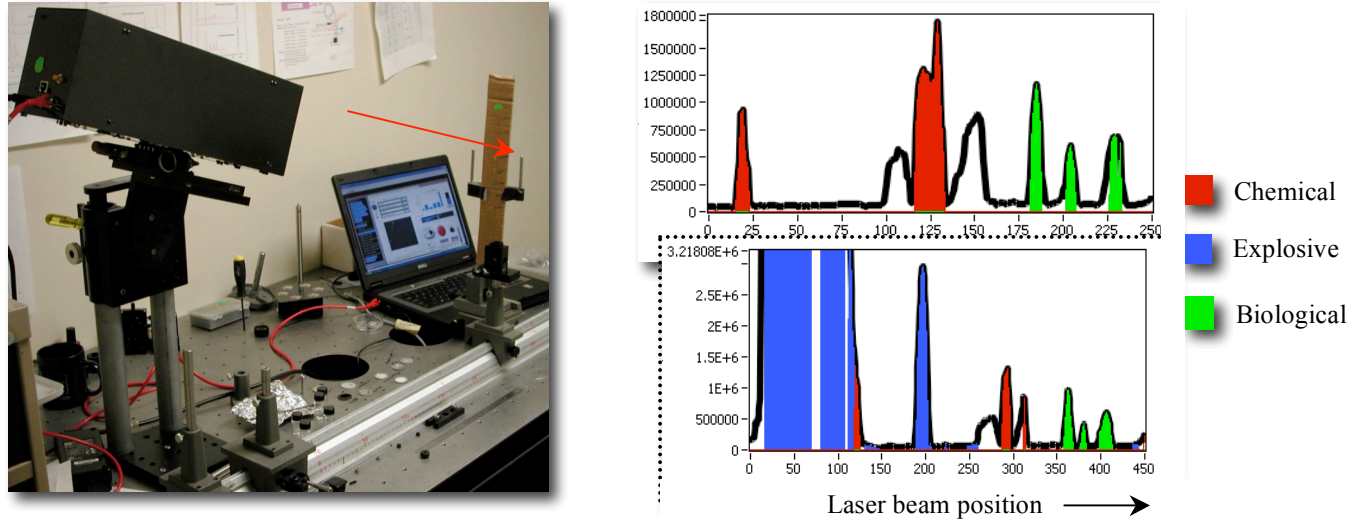
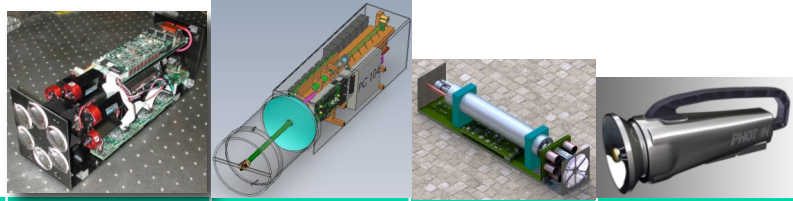


Fig. 6. Photo of scanning TUCBE sensor (right) with chemical relationship (color) or non-relationship (no-color) (left)

As the sensor laser beam is scanned over the cardboard target with dopants, the chemical identity is constantly being determined and related to an internal data base. In the case shown here, only the coarsest classification of the detected substance is identified. The black outline represents the amplitude of the combined signal measured in all spectral bands. If no color was associated with a signal, no chemical identity could be defined. More specific identity could have been attributed to each data point than is shown here, but the level of identity could be a source of confusion unless the operator is skilled in chemical nomenclature. Fig. 6 illustrates just one example of how a display of hazard could be presented. Another display being developed is a list of the most likely identity of all the materials in the data base, listed according to the scalar distance in chemometric space to the unknown sample being detected. We are developing a chemical vectoring approach to identifying materials based on their chemometric signature and their temporal and spatial histories.

Above are data on the Gen 1.0 TUCBE sensor that demonstrated the ability to detect and classify explosive and biological materials at a level of 100 ng/cm^2 and $100 \text{ bacterial spores/cm}^2$ at a working distance of 1 m. The signal to noise (S/N) ratio for these measurements was typically over 50:1. At higher concentrations working distances could be proportionally extended so that at 500 ng/cm^2 of explosives the working distance would be about 5 m. Conversely, at shorter working distances, the Gen 1.0 TUCBE sensor could sense smaller concentrations of hazardous materials. The Gen 1.0 sensor was a proof of concept sensor and did not have several features of importance to a fieldable sensor for robot or hand-held applications. First, the data processing computer was not imbedded in the sensor. It is shown in Fig. 6 as a separate notebook computer, linked to the sensor with a wireless link. Therefore the sensor could not be operated using the robot operating system and, in addition, the software was not compatible with robot operating systems: JAUS. Second, the Gen 1.0 sensor did not have a visible aiming beam to help identify the target at which the sensor was pointed. It was difficult therefore to have spatial context to the chemical information and mapping a target area was difficult without the image context. Finally, the working distance was not optimized for the sensor and more performance could be obtained with minimal addition of weight and size. Therefore an imbedded data processing computer, visible aiming beam, and higher efficiency collection optics were considered necessary for future generations of the TUCBE sensor. These generation changes are illustrated in Table I, below, where the basic feature of each generation is described.

Table I: TUCBE generation differences



Description	Gen 1.0 May 07	Gen 1.5 Sept. 08	Gen 2.0 Sept. 09	Gen 2.0+ Feb. 10?
Standoff distance at 100ng/cm ² explosives & 100 spores/cm ²	1 - 2 m	3 - 5 m	3 – 5 m	3 to 10 m
Data processing	Remote	Internal	Internal	Internal
Visible aiming beam	No	Yes	Yes	Yes
Interface	Robot	Robot	Robot	Hand-held
Ruggedized	No	Yes	Yes	Yes
Size	5"x6"x14"	3"x4"x16"	3"x3"x14"	3"x4"x15"
Weight	5 lb	7.5 lb	< 5 lb	6.6 lb
Power	Robot	Robot	Robot	On-board batterv
J AUS Compliance	No	Yes	Yes	Yes

3. DEEP UV RAMAN AND LASER INDUCED NATIVE FLUORESCENCE

Deep UV optical sensors for detecting and classifying or identifying CBE materials UV have several advantages over sensor operating in the visible or near-IR, or other types of sensors. These advantages are summarized as:

1. Clear Raman spectra with no obscuration or interference by native fluorescence from the target or surrounding materials
2. The ability to simultaneously detect Raman and native fluorescence emissions from target materials
3. Much higher sensitivity due to Rayleigh law and resonance Raman signal enhancements
4. Simplification of Raman spectra due to resonance effects
5. Solar blind detection of Raman and fluorescence because of short operating wavelength
6. Low thermal noise compared to IR detection
7. Non-contact, non-destructive, no sample handling
8. Reagentless
9. Reduced eye hazard

Raman scattering is a far less efficient process than Rayleigh scattering or fluorescence. Therefore if any fluorescence process occurs within the target molecules or surrounding materials within the exposure volume of the excitation laser beam, it will overwhelm the weak Raman emissions. For excitation in the visible or near IR, the fluorescence efficiency of many materials is over 10⁴ to 10⁸ times greater than Raman scattering efficiency. It is commonly accepted practice to move to the near IR to avoid fluorescence, but with excitation even as high as 830 nm, it has been shown that a large fraction of materials investigated exhibit major fluorescence interference[1] to the point that it completely obscures Raman emissions. Even in the deep UV fluorescence is still at least 5000 to 10000 times greater than Raman scattering, unless excitation occurs below about 250nm. Asher[2],[3] showed that organic materials did not fluoresce below a wavelength about 270nm, independent of the excitation wavelength. This was further proven in many subsequent publications such as Nelson[4], Sparrow[5], Wu[6], and many others. Therefore, when excitation occurs below about 250nm, a fluorescence-free region extends from the excitation wavelength to over 4000 cm⁻¹ in which to observe

Raman spectra. This is not the case for lasers that provide excitation at longer wavelengths. Even excitation at 266nm from a 4th harmonic Nd-YVO₄ laser, or equivalent, has most of its Raman spectral range overlapped with fluorescence from a wide range of organic and mineral materials as illustrated in Fig. 7[7].

When excitation occurs in the deep UV below about 250nm, Raman and fluorescence emissions from target materials occur in different wavelength regions, allowing for simultaneous collection of Raman and fluorescence information and improving the chemical specificity with which targets can be identified. Asher (Ref. 8) showed that the range of emission wavelengths due to these processes is generally limited to wavelengths above about 260nm. Essentially no materials fluoresce or phosphoresce below this wavelength. Raman spectra, on the contrary, are dependent on the excitation wavelength and are measured in molecular vibration energy terms above (Stokes) or below (anti-Stokes) the excitation wavelength. Therefore, as the excitation wavelength is reduced below the lower limit of fluorescence, there is a fluorescence-background-free region above the excitation wavelength in which to observe the normally weak Raman emissions. This is graphically illustrated in Figure 7, below.

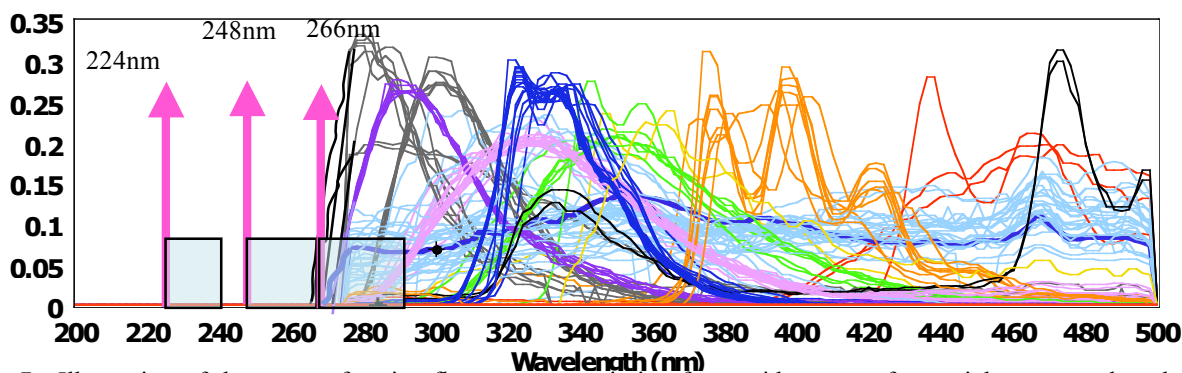


Fig. 7. Illustration of the range of native fluorescence emission for a wide range of materials compared to deep UV Raman emission ranges with excitation at 224nm, 248nm, and 266nm lasers

The pale blue band above each of the excitation wavelengths shown in Fig. 7 correspond to a 3000 cm^{-1} Raman shift range. Illustrated is the fact that excitation at 224nm provides a fluorescence-background-free range for well over 3000 cm^{-1} . Excitation at 248nm is fluorescence-background-free for all but a few materials, and only at the largest Raman shifts. Excitation at 266nm occurs directly in the middle of the native fluorescence of a wide range of biological and organic chemical materials. In addition, the water Raman band for a 266 nm laser occurs in the middle of biological native fluorescence bands, making it difficult to use this excitation wavelength for biological identification using native fluorescence. Excitation at longer wavelengths further exacerbates the problem of fluorescence interference, just as the Raman signals themselves are diminished by Rayleigh law and resonance or pre-resonance effects.

Since the Raman and native fluorescence emission bands are separated with deep UV excitation, it is therefore ideal to combine UV Raman and native fluorescence to form an integrated tool for detection and identification of CBE materials since these methods offer a great combination of sensitivity and specificity that do not share overlapping observation wavebands and both modes of detection can be employed simultaneously.

In addition to virtual elimination of fluorescence background, operation in the deep UV enables Raman signal enhancement due to both Rayleigh scattering and resonance effects. Raman scatter cross section of any material depends as the inverse fourth power on excitation wavelength, called the Rayleigh scattering law. The Raman cross-section of any Raman band is 20X larger at 248nm than at 532nm and 100 times larger than at 785nm. Overlaid on this signal improvement are pre-resonance or resonance effects which can provide additional increase in Raman cross-sections by factors up to several million times. Between excitation at 532 nm and 248 nm pre-resonance effects for water increase the Raman cross-section about 6X for a total Raman cross-section increase due to Rayleigh and pre-resonance of 120X. The Raman cross-section of water, including both Rayleigh and pre-resonance effects, is 570X between 785 nm and 248 nm. This means that a 785 nm laser requires 570X more power to achieve the same Raman signal as a 248 nm laser.

Over the past fifteen years UV resonance Raman spectroscopy has been increasingly used for detection and identification of microorganisms and study of cellular function[8],[9],[10],[11],[12]. It has been clear for several years that unique ultraviolet resonance Raman spectral signatures can reliably be detected in as few as 20 bacterial cells with low power consumption and low photon flux levels (Nelson, 1993[13]; Nelson, et.al.[14], 1993; Chadha, et.al., 1993[15]. Identification of biopolymers or organisms using UV Raman spectroscopy depends on the ability to produce interpretable, reproducible spectra. DNA and cell surface antigens are the most attractive targets as potential markers for cellular or bacterial identification. Identification of organisms using UV Raman spectroscopy has focused on the ratio of a few taxonomic marker bands. These band markers are based on ratios of tryptophan and tyrosine and DNA base pairs that can be characteristic of an organism. As mentioned previously, most biological materials have repeating functional groups that are highly degenerate. These include nucleic acid base pairs and aromatic amino acids. These repeating units have Raman spectra that are very similar to the spectra of the monomers upon which they are based. A summary of the major taxonomic marker bands of highly degenerate functional groups occurring within microorganisms is shown below in Table II below with the major marker band is bold. Explosives also have specific marker bands that can be used to distinguish these materials from interferants. A dominant marker band for explosives is at 1365 cm^{-1} , which distinguishes ammonium nitrate from HMX, RDX, PETN, and nitrocellulose[16].

Table II. Major Taxonomic Raman marker bands for biological agents

Material	Raman Marker Band Locations					
Tryptophan	753	879	1011	1353	1555	1615
Tyrosine	831	852	1180	1210		1615
Guanine				1320 1365	1485	1577 1603
Adenine				1337	1485	1580
Cytosine					1530	
Dipicolinic Acid			1017	1195	1396	1446

Figure 8, below, illustrates the ability to distinguish different materials using native fluorescence alone, where bacterial spores and cells and explosives materials (group E) occupy clearly different regions of chemometric PCA space.

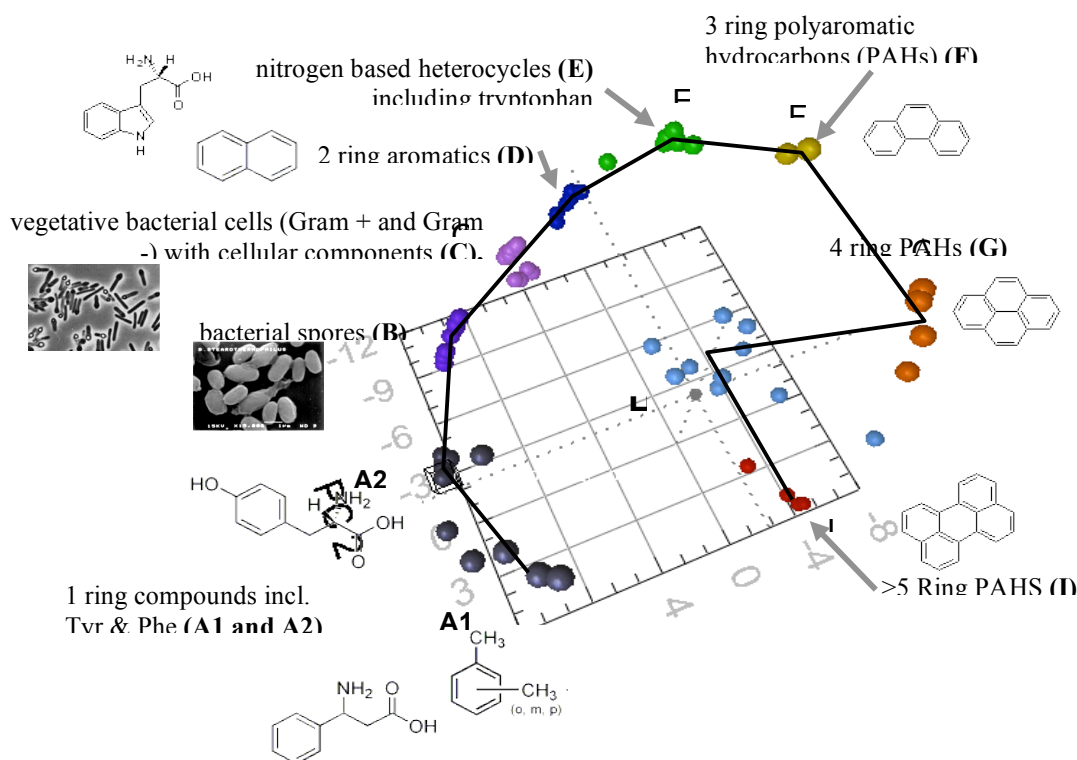


Fig. 8. Differentiability of bacteria, explosives and other materials using native fluorescence alone. Ex = 235 nm.

The ability to differentiate these materials is strongly dependent on excitation wavelength[17]. Fig. 8 illustrates the best differentiability with an excitation wavelength of 235 nm. As excitation wavelength is increased above about 250 nm the ability to differentiate diminishes dramatically. The differentiability illustrated in Figs. 4 and 5 was accomplished with an excitation wavelength of 248 nm. Although Fig. 8 illustrates the ability to distinguish mixed materials such as bacterial spores and cells from pure materials, we have, in addition, developed a method of chemical vectoring to deal with complex mixtures and composite materials. Excitation of CBE materials at longer wavelength typically does not excite core materials in these agents. Excitation at 375 nm with semiconductor lasers typically only observes growth media when looking at bacterial spores, and does not detect intrinsic biological material.

4. ENABLING TECHNOLOGIES

The core technologies that enable the TUCBE sensor are a new class of ultra-narrow-band deep UV lasers emitting at either 224.3 nm or 248.6 nm as well as new gated, high etendue, marker band detection and chemometric methods. Few deep UV laser types have the potential for miniaturization that also provide the emission wavelengths and linewidth needed for Raman. They include transverse excited hollow cathode (TEHC) lasers as well as fifth harmonic diode pumped solid-state (DPSS) lasers and potentially a new generation of semiconductor lasers being developed by Photon Systems under DARPA and more recently NASA sponsorship.

The only currently available lasers which satisfy size, weight, power consumption and cost constraints of these hand-held sensors are the 224.3nm 248.6nm lasers developed by Photon Systems. Versions of these lasers with overall



Figure 9. Photo of TEHC laser

length about 30cm emit over 100mW at 248.6nm during their on time, have an emission linewidth less than 0.1cm^{-1} , operate with stable emission wavelength at ambient temperatures below -100°C without any preheating or temperature regulation, operate at very high duty cycles (10^{-2}) and are very compact and efficient compared to other presently available sources. These lasers have successfully undergone shock and vibration testing to the NASA Mars Science Laboratory launch and landing specifications and have been tested and operated at temperatures to -80°C without warm-up, preheating or temperature regulation. Only our test chamber limited the temperature of testing. Because of the very narrow linewidth and stable emission wavelength, these sources make ideal sources for deep UV resonance Raman spectroscopy and surface-enhanced resonance Raman spectroscopy. The lasers employ all metal-ceramic construction, similar to miniature klystrons or traveling wave tubes. Laser weight is less than 1 lb and power consumption is less than

5 W including 4 W of housekeeping power at a data accumulation rate of 10 Hz. These lasers are hundreds to thousands of times smaller, lighter, less power consumption, and cost compared to other deep UV lasers on the market. And DHHS/CDRH rates these lasers as Class I on single pulse basis and Class IIIb on a multiple repetition basis. Typical penetration depth into target materials is less than a few micrometers. Therefore, damage to a retina or lens is not possible.

The TUCBE sensor employs a very high etendue optical system that makes the sensor insensitive to shock and vibration since there are not critical alignment features of the optical system. Although the laser is a CW laser, the output is commutated by the drive electronics with digitally controlled pulse widths from $30\ \mu\text{s}$ to $100\ \mu\text{s}$, producing an emission typically over 10^{14} photons/pulse. The detection system employs miniature, metal can, photomultiplier tubes (PMTs) with digitally controlled PMT controllers with gated boxcar integrators, developed by Photon Systems. Detection electronics have a linear dynamic range over 10 decades, allowing detection of weak Raman emissions of a few photons up to large fluorescence emissions of 10^{10} photons in a single digital laser pulse. Detection electronics have the following other features: Synchronizes detection with laser pulse; Integrates collected photons into computer selected capacitors of 33pf, 470pf, & 4700pf; Digitally adjustable start/finish signal integration, 1us resolution; Digitizes capacitor charge into detection "counts" at the end of integration period; Computes incident photons, independent of gain and capacitor setting, based on on-board calibrated capacitance and look-up-table of absolute PMT gain versus PMT voltage; Each detector is serialized along with custom data; few photon counting in deep UV; 32 bit, 75 Mips processor with 2M RAM and 256K flash; 16 bit A/D with 16 bit resolution; Built in capacitor calibration and test; USB

or Ethernet interface; control by LabView. Automatic gain control and background subtraction features of the TUCBE sensor allow on-the-fly compensation of signals while scanning over widely disparate natural environments.

5. OTHER APPLICATIONS

The TUCBE sensor has a wide range of applications other than military or homeland security. As a surface detector the TUCBE sensor or its variants can precisely measure quality of manufactured products including pharmaceuticals, food, and other chemicals and semiconductor materials in on-line production facilities. In addition, these sensors have been configured for municipal, industrial, agricultural, and potable water quality measurements where the sensors have demonstrated the ability to detect and classify bacteria, virus' and other biological materials with a limit of detection less than 10 spores or virus' per mL. We have also demonstrated the ability to distinguish various strains of bacteria.

6. ACKNOWLEDGEMENTS

Photon Systems gratefully acknowledges the support of this present effort by U.S. Army STTR contract No. W81XWH-06-C-0395 as well as previous and ongoing support for related developments by NASA, JPL, DARPA, and EPA.

7. REFERENCES

- [1] Frosch, T., et.al. UV Raman Imaging, A promising tool. *Anal. Chem.* Vol.79, No.3, (Feb. 1, 2007)
- [2] Asher, S.A., and C.R. Johnson, "Raman Spectroscopy of a Coal Liquid Shows That Fluorescence Interference Is Minimized with Ultraviolet Excitation", *Science*, 225, 311-313, 20 July (1984).
- [3] Asher, S.A. and C.R. Johnson, "UV Resonance Raman Excitation Profile Through the 1B_2 State of Benzene", *J. Phys. Chem.* Vol. 89, pp. 1375-1379 (1985).
- [4] Nelson, W.H., R. Manoharan and J.F. Sperry, "UV Resonance Raman Studies of Bacteria", *App. Spect. Reviews*, 27 (1), pp67-124, (1992)
- [5] Sparrow, M.C., J.F. Jackovitz, C.H. Munro, W.F. Hug, and S.A. Asher, "A New 224nm Hollow Cathode UV Laser Raman Spectrometer", *App. Spect.*, Vol. 55, No. 1, Jan (2001).
- [6] Wu, M., M.Ray, K.H.Fung, M.W. Ruckman, D. Harder, and A.J. Sedlacek, "Stand-off Detection of Chemicals by UV Raman Spectroscopy", *App. Spect.*, Vol.54, No.6, pp. 800-806 (2000).
- [7] Hug, W.F., R. Bhartia, A. Tsapin, A. Lane, P. Conrad, K. Sijapati, and R. D. Reid, "Water & surface contamination monitoring using deep UV laser induced native fluorescence and Raman spectroscopy", *Proc. SPIE*, Vol. 6378, Boston, MA. Oct. (2006).
- [8] Nelson, W.H., R. Manoharan and J.F. Sperry, "UV Resonance Raman Studies of Bacteria", *App. Spect. Reviews*, 27 (1), pp67-124, (1992)
- [9] Chadha, S., W. H. Nelson and J.F. Sperry, "Ultraviolet micro-Raman spectrograph for the detection of small numbers of bacterial cells", *Rev. Sci. Instrum.* 64 (11), pp.3088-3093, Nov. (1993)
- [10] Chi, Z., and S. A. Asher, "UV resonance Raman Determination of Protein Acid Denaturation", *Biochemistry*, 37, pp.2865-2872, (1998).
- [11] Cho, N., and S.A. Asher, "UV resonance Raman studies of DNA-Pyrene interactions", *J.Am. Chem.Soc.* 115, pp.6349-6356, (1993)
- [12] Sureau, F., et.al., "An ultraviolet micro-Raman spectrometer: Resonance Raman spectroscopy within a single cell", *App.Spect.*, 44, No.6, pp.1047-1051, (1990)
- [13] Nelson, W.H. *Rev. Sci. Inst.* (11):3088-3093 (1993)
- [14] Nelson, W.H. , Manoharan, R., and Sperry, J.F. *Appl. Spect. Rev.* 27(1), 67 (1992)
- [15] Chadha, S., Nelson, W.H., Sperry, J.F. *Rev. Sci. Inst.* (11):3088-3093 (1993)
- [16] Gardner, C.W., et.al. Demonstration of a Robot-Based Raman Spectroscopic Detector for the Identification of CBE Threat Agents, 25th Army Science Conference, (2006)
- [17] Patents have been applied for related to this sensor method and wavelength dependence